J. Phys. B: At. Mol. Opt. Phys. **33** (2000) 5387–5395. Printed in the UK PII: S0953-4075(00)50247-8

Absolute emission cross sections for electron capture reactions of C^{2+}, N^{3+}, N^{4+} and O^{3+} ions in collisions with Li(2s) atoms

G Rieger†, E H Pinnington† and C Ciubotariu‡

† Department of Physics, University of Alberta, Edmonton, Alberta, Canada T6G 2J1
‡ Physics Department, University of Lethbridge, Lethbridge, Alberta, Canada T1K 3M4

Received 22 February 2000, in final form 26 July 2000

Abstract. Absolute photon emission cross sections following electron capture reactions have been measured for C^{2+}, N^{3+}, N^{4+} and O^{3+} ions colliding with Li(2s) atoms at keV energies. The results are compared with calculations using the extended classical over-the-barrier model by Niehaus. We explore the limits of our experimental method and present a detailed discussion of experimental errors.

1. Introduction

In this work we look at collisions between ions and lithium atoms in the ground state. This is not only of fundamental interest but the cross sections also have an important application in fusion plasma diagnostics. For this purpose, a compilation of cross section data for various inelastic processes in collisions between electrons or ions with lithium atoms has recently been published by Wutte *et al* (1997). In assessing the available data the authors gave preference to 'experimental data of the highest accuracy, judged by the inherent potential for the applied experimental method to generate accurate cross sections and by the care exercised to specify all the error sources in the measurement'. The last point is especially important since many parameters are involved in a cross section measurement that need careful control. In the following sections we investigate the different error contributions of our experimental method and report the first absolute emission cross sections obtained with the Alberta ECR ion source.

2. Experiment

2.1. Experimental set-up

The experimental set-up is typical for the study of atomic collisions using photon spectroscopy as the method of detection. Such experiments have been described many times in the past (e.g. Aumayr *et al* 1984, Dijkkamp *et al* 1984), so we will present just the main features.

The highly charged ions are produced in a source based on electron cyclotron resonance at 10 GHz similar to the MINIMAFIOS type (Geller and Jacquot 1983). Typical beam currents measured behind the interaction region are about 0.5–1.0 μA. The size of the beam is limited by apertures to 6 mm in diameter in the target chamber where the ions are crossed with a perpendicular beam of lithium atoms. The lithium vapour is produced in a single-stage oven based on resistive heating using a stable current source. Typical powers applied to the

0953-4075/00/235387+09$30.00

oven were about 70–80 W, yielding temperatures in the range 450–500 °C measured with a thermocouple. The target density is about 10^{11} cm^{-3}, ensuring single-collision conditions. The beam emerges through a capillary of 1 mm diameter and 5 mm length in the top lid of the oven and is additionally limited by apertures to a diameter of 6 mm in the interaction region. The lithium beam can additionally be excited in the interaction region with light from a diode laser (TUI-lasers, model DL 100) tuned to the Li(2s–2p) resonance line at 670.8 nm. In the present experiment, the laser-induced fluorescence (LIF) detected by a photodiode (Hamamatsu S1406) is used to monitor the stability of the Li-target density.

The charge transfer reactions are observed using photon emission spectroscopy in the region 260–800 nm. A quartz lens projects the interaction region onto the entrance slit of a 0.3 m monochromator (McPherson 218) that is at an angle of 54.7° with respect to the ion beam direction (magic angle) and tilted by 45° to avoid errors due to polarization effects on the measured cross sections. The monochromator is equipped with a photomultiplier (Hamamatsu 943-02) in a cooled housing reducing noise levels to less than 5 counts/s. The slits were opened to 0.4 mm during the experiments leading to a typical linewidth of 0.5 nm (FWHM).

2.2. Calibration and determination of emission cross sections

The measured signal or intensity $S(\lambda_{if})$ of a spectral line is related to the emission cross section $\sigma(\lambda_{if})^{\mathrm{em}}$ by (Aumayr *et al* 1984)

$$S(\lambda_{if})^{\mathrm{em}} = \sigma(\lambda_{if})^{\mathrm{em}} \frac{\Omega}{4\pi} P k(\lambda_{if}) \frac{Q}{q} n_0 L \frac{1}{C_i} \tag{1}$$

where Ω is the solid angle of the detection system, P is a correction factor for the polarization of the emitted radiation ($P = 1$ in our case), $k(\lambda_{if})$ is the detection efficiency at wavelength λ_{if}, Q is the total accumulated charge, q is the charge state of the projectile, n_0 is the target density (assumed to be uniform) and L is the observation length, which is 12 mm in our experiment. The factor $1/C_i$ is the lifetime-correction factor which is important in the case that the electron is captured into an excited state having a lifetime that is longer than the time the ions spend in the observation region.

In order to obtain absolute emission cross sections from the measured signal, we calibrate our data against the cross section for Li(2s–2p) emission due to proton impact measured with good precision (8% total error) by Aumayr *et al* (1984). Provided that the known emission cross section for the excitation of Li due to proton impact, $\sigma(670.8)^{\mathrm{em}}$, is measured under the same conditions as the emission cross section due to charge transfer of an electron to a highly charged ion, $\sigma(\lambda_{if})^{\mathrm{em}}$, the latter can be obtained from the signals and ion beam currents measured in the two experiments:

$$\sigma(\lambda_{if}) = \frac{S(\lambda_{if})}{S(670.8)} \frac{Q(\mathrm{H}^+)}{Q(\mathrm{A}^{q+})} \frac{\mathrm{RI}(670.8)}{\mathrm{RI}(\lambda_{if})} q(\mathrm{A}^{q+}) \sigma(670.8)^{\mathrm{em}}. \tag{2}$$

Here, $S(\lambda_{if})$ is the signal measured for the capture reaction and $S(670.8)$ is the signal for the Li excitation, $Q(\mathrm{H}^+)$ and $Q(\mathrm{A}^{q+})$ are the measured integrated beam currents for the proton beam and the beam of the ion used in the capture experiment, and $q(\mathrm{A}^{q+})$ is the charge state of the ion used in the capture experiment. The absolute detection efficiencies are replaced by relative intensities at the corresponding wavelengths, RI(670.8) and RI(λ_{if}), since the same monochromator is used for all experiments under the same geometric conditions which also eliminates the solid detection angle from the equation.

The lifetime correction factor is neglected in equation (2) since it was negligible in most cases. However, it had to be introduced in the cases of the 3s–3p and 3p–3d transitions in

N III, the 3s–3p transition in N IV, and the 3s–3p transition in C II. The corresponding lifetimes and ion velocities led together with our observation length of 12 mm to a correction of the emission cross section in the range between 3% and 29%. We used transition probabilities from the NIST atomic spectra database (ASD) (http://www.physics.nist.gov) for the calculations of lifetimes and branching ratios. Equation (2) can be used as long as the target density does not change between the capture experiment and the excitation experiment.

2.3. Error sources and experimental limits

Experimental charge transfer cross sections typically have an error of at least ±30% or more. The measurement of the emission cross section of Li(2s–2p) excitation due to proton impact to a total error of ±8% by Aumayr *et al* (1984) can therefore be considered as a high-precision measurement. As we use their results to put our cross sections on an absolute scale, this error adds to all other errors in our experiment.

In order to minimize the experimental error, each cross section result consists of several (typically nine) measurements. For each cross section measurement, a separate calibration experiment was performed, i.e. a measurement of the photon emission spectrum for Li excitation due to proton impact. The measurements were repeated on different days to check for systematic drifts. Small differences in position, focusing and shape of the ion beam should therefore be statistically distributed and are accounted for in the statistical error. In this way, we detected an error source not discussed in the literature so far, which is contamination of the target beam. Contamination of the target will lead to a systematic overestimation of our experimental emission cross because our calibration method is only sensitive to the lithium density. Contamination is significant shortly after refilling the oven with lithium and disappears typically after three to four days of pumping at a moderate oven temperature (250 °C). A visible signature of contamination is the appearance of hydrogen lines in our spectra. The long time to obtain a clean target beam is probably due to a combination of the small capillary through which the volume of the oven must be pumped and the lower pumping speed for hydrogen.

The relative intensities were measured with good accuracy in the range 300–700 nm where we estimate the error to be less than ±5%. However, below 280 nm the calibration curve has a quickly increasing error due to the poor UV-yield of the calibrated lamp and the low efficiency of the grating (blazed for 500 nm). The measurement of the 264 nm line of N^{4+} is heavily affected by this. The error in the relative intensity at this wavelength might be as much as ±50%.

Errors due to the beam current measurement are negligible in comparison with those due to other sources discussed here. Since our ion source produces a proton beam at the same time as the highly charged ions, the beam geometry does not change and capture and the excitation experiments can be performed within a short time interval. However, it is important that the overlap between the ion beam and target does not change between cross section and calibration experiments. We minimized such an error by using apertures to limit the size of the ion beam from originally about 2 cm in diameter to 6 mm in the interaction region. The ion beam profiles appeared to be uniform over the 6 mm diameter.

Target density fluctuations are problematic if they occur over a short time, especially between calibration measurements (Li excitation due to proton impact) and the emission cross section measurement of interest. We measured these fluctuations using a diode laser tuned to the Li(2s–2p) resonance line and measured the laser-induced fluorescence on a photodiode. Once the oven temperature was stable (about 2 h after switch-on), the measured fluorescence did not change by more than ±5% over the following 6 h and no rapid changes were observed. Errors due to target density fluctuations are therefore believed to be small and are taken into

account by the statistical error.

It is well known that an ECR ion source produces significant fractions of ions in a metastable state. If the lifetime is sufficiently long (>10 μs) those states survive into the interaction region. As charge transfer reactions are core-conserving, transitions in two different term systems due to the ground-state projectiles and the metastable projectiles are observed. Consequently, only a part of the ions in the beam contributes to the intensity of each spectral line, either the metastable fraction or the ions in the ground state. Thus experimental cross sections have to be corrected for metastable fractions, but we were not able to measure the metastable fractions f produced by our ion source. Therefore, we used the following experimental values to correct our cross sections: $f = 0.56$ for C^{2+} ions, $f = 0.52$ for N^{3+} ions (both Brazuk *et al* 1984b), and $f = 0.12$ for O^{3+} ions (Beijers *et al* 1996). The emission cross sections for O^{6+} ($f = 0.01$, Folkmann *et al* 1983) and N^{4+} (no metastable state) were not corrected.

The use of literature values for the metastable fraction is certainly problematic and may lead to large errors in our experiment. For example, Greenwood *et al* (1996) measured metastable fractions between 0.25 and 0.45 source for C^{2+} projectiles produced by their 5 GHz ECR source while Brazuk and co-workers (1984b) measured a fraction $f = 0.56$ produced in a 10 GHz ECR source. Brazuk and co-workers report that their results (supported by calculations) do not significantly depend on the source parameters used in contrast to Greenwood *et al*. We decided to use the values of Brazuk and co-workers (1984b) and Beijers *et al* (1996) since their results were obtained with an ECR source that is similar to ours. We have included a possible systematic error of $\pm 50\%$ in the final estimates of the cross section for C^{2+} and N^{3+} projectiles to allow for the uncertainty of the ions in the metastable state. Since the metastable fraction is certainly much lower in the case of O^{3+} projectiles, the included systematic error is only $\pm 10\%$. We also report 'uncorrected' errors in our results (tables 1 and 2) where this systematic error is not included. Our values may be adjusted later and the total error reduced in the case that an independent measurement of our cross sections allows an estimate of the actual metastable fraction in our experiment. This uncorrected error in our measurements of emission cross sections consists of the statistical error, the error in the relative intensities and the error quoted by Aumayr *et al* (1984) for the emission cross section of Li excitation due to proton impact.

3. Results and discussion

3.1. Results

Table 1 shows the emission cross sections for all lines measured at different energies. We also measured the emission cross section of the 6g, h–7h, i transition in O VI in collisions between O^{6+} ions and Li atoms. This cross section has been measured before by Brazuk *et al* (1984a) and we chose the same collision velocity of $v = 0.41$ au to allow a comparison of the two results. Our value of 14.6×10^{-15} cm^2 (total error of $\pm 27\%$) is in good agreement with the result obtained by Brazuk and co-workers (12.6×10^{-15} cm$^2 \pm 40\%$) within the error bar of either experiment. This gives us confidence that our experimental approach yields reliable results.

The emission cross sections in table 1 correspond to the strongest lines in each spectrum in the observed wavelength region following single-electron capture. Which energy levels are populated by the charge exchange depends mostly on the energy of the populated state in the projectile and the ionization potential of the target. The collision energy is another important parameter. We varied the acceleration potential in the range 6–12 kV for most of the lines without expecting the cross sections to change significantly over this small range.

Table 1. Measured emission cross sections. The total error includes a possible systematic error in the metastable beam fraction of ±50% in the case of C^{2+} and N^{3+} projectiles and ±10% in the case of O^{3+} projectiles (see text). Error values not including this systematic error are given in parentheses.

Inc. ion	E (keV)	λ (nm)	Transition	σ^{em} (10^{-15} cm^2)	Total error (%)
C^{2+}	12	427	C^+:	0.7	±72 (±22)
	18		3d ^{2}D–4f ^{2}F^o	1.0	±90 (±40)
	24			0.9	±99 (±49)
	12	589	C^+:	1.4	±81 (±31)
	18		3d ^{2}D–4p ^{2}P^o	3.2	±76 (±26)
	24			1.6	±100 (±52)
	12	658	C^+:	2.3[a]	±69 (±19)
	18		3s ^{2}S–3p ^{2}P^o	2.9[a]	±76 (±26)
	24			3.3[a]	±93 (±43)
N^{3+}	27	410	N^{2+}: 3s ^{2}S–3p ^{2}P^o	2.8	±84 (±34)
	27	438	4f ^{2}F^o–5g ^{2}G	0.7	±91 (±41)
	27	451	3s ^{4}P^o–3p ^{4}D	2.8	±80 (±30)
	27	486	3p^{4}D–3d ^{4}F^o	1.5	±80 (±30)
N^{4+}	36	265	N^{3+}:	2.9	±54
	48		4f ^{3}F^o–5g ^{3}G	2.4	±56
	24	348	N^{3+}:	11	±54
	36		3s ^{3}S–3p ^{3}P^o	18	±31
	48			16	±53
	24	460	N^{3+}:	1.9	±25
	36		5g ^{3}G–6h ^{3}H^o	1.7	±21
	48			2.8	±34
O^{3+}	18	326	O^{2+}:	2.3	±26 (±16)
	27		3p ^{3}D–3d ^{3}F^o	2.5	±26 (±16)
	36			2.6	±20 (±10)
	18	375	O^{2+}:	4.5	±24 (±14)
	27		3s ^{3}P^o–3p ^{3}D	4.5	±29 (±19)
	36			3.7	±27 (±17)

[a] Represents an upper limit as cascades were neglected (see text).

A simple model that is based on energies is the extended classical over-the-barrier (ECB) model by Niehaus (1986). We used the ECB model to estimate cross sections for the capture into excited states of the projectiles. Although details of the collision system such as spin are not taken into account, the model is still useful to gain first insights into a reaction. We compare the predictions of the ECB model to our experimental capture cross sections using the experimental emission cross sections and taking into account branching ratios and cascades when necessary. The results are presented in table 2. While the ECB model correctly predicts the preferentially populated levels, only an approximate agreement between experimental and calculated values of the capture cross sections is obtained. However, this is not surprising given the simplicity of the model.

We measured the spectra (except N^{3+}–Li) at three different projectile energies in the range 6–12q kV but the variations cannot be regarded as significant since the differences are within the experimental error bars. This is also supported by the ECB model that predicts changes of less than 10% in the capture cross sections for our energy range. We have therefore included a mean value of the cross sections measured at different energies in table 2. This value can be considered as our best estimate for the cross sections measured in our energy range. In

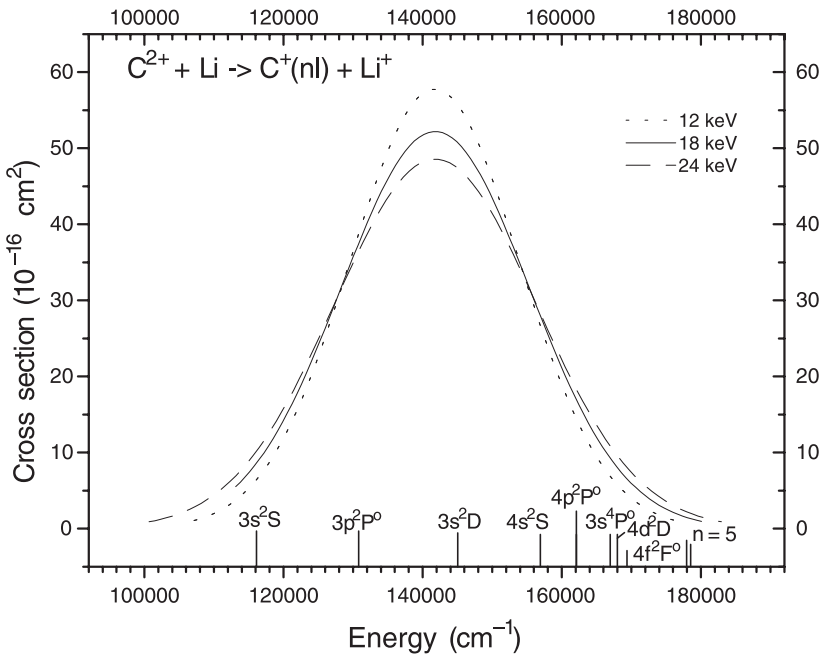

Figure 1. Calculated single-electron capture cross section for the C^{2+}–Li collision system using the ECB model (Niehaus 1986). The cross section is plotted as a function of the binding energy of the transferred electron in the projectile for three different projectile energies. The approximate positions of some energy levels discussed in the text are indicated.

We calculated estimates of the cross sections for electron capture into the 4f $^2F^o$, 4p $^2P^o$ and 3p $^2P^o$ levels (see table 2) from the appropriate emission cross sections taking into account the branching ratios of the transitions. Cascades were neglected which is a problem only in case of the 3p state where the repopulation from the $n = 4$ level may be significant. We could not measure the corresponding transitions so the measured cross section represents only an upper value for capture into 3p.

3.3. Single electron capture by N^{3+} ions into $N^{2+}(nl)$ states.

About half of the N^{3+} ions in our beam are in the metastable $N^{3+}(1s^22s2p\ ^3P^o)$ state. Thus capture into doublet and quartet states of $N^{2+}(nl)$ is expected and is indeed observed. Capture by $N^{3+}(1s^22s^2)$ ions leads to $N^{2+}(1s^22s^2nl\ ^2L)$ states. The ECB model predicts capture predominantly into $n = 4$ and to a lesser extent the $n = 5$ levels. The 4f–5g transition is the only transition from an $n = 5$ level we measured and it should also be the strongest one (statistical distribution of the population of l-states, branching ratio $= 1.0$). The measured emission cross section is also our estimate of the capture cross section into the 5g level neglecting a possible but presumably very small cascade from the 6h level. Transitions from $n = 4$ cannot be observed with our equipment as the corresponding wavelengths are below 250 nm. Since the population of the 3p state is mainly due to cascades, no estimate for capture into this state is given in table 2.

Capture by the metastable $N^{3+}(1s^22s2p\ ^3P^o)$ ions lead to $N^{2+}(1s^22s2p\ ^3P^o\ nl\ ^2L,\ ^4L)$ states. It is interesting to note that only transitions in the quartet term scheme are observed, although the population of doublet states is energetically possible as well. This effect has been

observed earlier and is partially explained by higher statistical weights of the quartet states. Transitions between doublet states are too weak to allow for a meaningful measurement of the cross section. In the quartet system the electron is captured into a doubly excited 3p or a 3d state. The ECB model predicts capture only into $n = 3$. Hence, cascades are neglected and the emission cross section for the 3p ^{4}D–3d ^{4}F^o transition is our estimate for the capture cross section into the 3d ^{4}F^o level (a branching ratio of 1.0). This transition has to be taken into account as a cascade when calculating the capture cross section for capture into the 3p ^{4}D level. The branching ratio of the 3s ^{4}P^o–3p ^{4}D transition is 1.0 so subtraction of the emission cross section of the 3p ^{4}D–3d ^{4}F^o transition from that of the 3s ^{4}P^o–3p ^{4}D transition yields the cross section for capture into 3p ^{4}D.

3.4. Single electron capture by N^{4+} ions into $N^{3+}(nl)$ states

The N^{4+}–Li collision system is not affected by metastable ions in the beam. Single electron capture leads to $1s^2 2snl\ ^{1,3}L$ states. States with $n = 5$ and 6 are in the energy region of the reaction window and should be preferentially populated. Due to the small beam current for N^{4+}, we observe only the strongest possible triplet transitions, i.e. the 5g–6h and the 4f–5g, both having a branching ratio of 1.0. Additionally, we observe the 3s–3p transition that is not populated by the capture process itself but due to cascades. Comparing the emission cross sections of the 4f–5g and the 5g–6h transitions one realizes that the emission cross section for the 4f–5g transition is underestimated because it is repopulated by the 5g–6h transition. Additionally, the 5g state is close to the maximum of the reaction window. Hence one would expect the 4f–5g emission cross section to be significantly bigger than the 5g–6h emission cross section. The reason for this discrepancy is in the large error in our calibration curve for the relative intensities in the region 250–280 nm. An estimation of the capture cross section is therefore only given for the 6h state. We assumed a branching ratio of 1.0 and no cascades as the population of states with $n = 7$ is presumably very small.

3.5. Single electron capture by O^{3+} ions into $O^{2+}(nl)$ states

The metastable fraction in the O^{3+} ion beam is only 0.12 (Beijers *et al* 1996) and no transitions between levels with the excited core (configurations: $1s^2 2s2p^2\ ^4$P $nl\ ^{3,5}L$) were observed in our spectra. Electron capture by O^{3+} ions having the core in the ground state leads to $1s^2 2s^2 2p(^2P^o)nl\ ^{1,3}L$ excited states with $n = 4$ being the preferentially populated level. $n = 5$ levels may be populated as well but with a much lower probability. Additionally, most transitions $4l$–$5l'$ are below 300 nm where the detection efficiency of our grating is low. The same is true for $3l$–$4l'$ transitions at even shorter wavelength.

The two observed transitions 3s–3p and 3p–3d cannot be populated directly by the capture process for energetic reasons thus the populations of the 3p and the 3d states are entirely due to cascades where the 3p–3d transition is one of the cascades to the 3s–3p transition. Hence, no experimental capture cross sections can be presented for this collision system. No transitions in the singlet term system were observed, which is another indication that the capture process favours a population of the higher-spin states.

4. Conclusion

We have measured emission cross sections for the strongest lines in the 260–800 nm wavelength region for charge transfer reactions in collisions between lithium atoms and C^{2+}, N^{3+}, N^{4+} and O^{3+} ions at keV energies. The observed lines could be qualitatively explained using the ECB

model by Niehaus (1986). The measurement of the emission cross section for the $6l$–$7l'$ transition in O VI has shown good agreement with a previous experiment performed by Brazuk *et al* (1984a), proving that our method is adequate.

Despite our effort to identify and reduce experimental errors, the uncertainty in our data is still relatively large. This is due to the many parameters involved in a collision experiment, each contributing to the experimental error. The fraction of metastable ions in our beam represents the most important error source in our experiment since we could not measure it and had to rely on published data. An independent measurement of our cross sections would allow an estimation of this fraction and therefore the reduction of the total error in the case of C^{2+} and N^{3+} projectiles. The results for N^{4+} projectiles that do not have a metastable state and O^{3+} ions that have only a small metastable fraction are therefore much more accurate.

In summary, we have identified all possible error contributions as requested by Wutte and co-workers (1997) for reliable data obtained from a collision experiment. We are confident that our results are accurate within the quoted error bars, which are in the range of similar subshell selective electron capture measurements.

Acknowledgments

This work has been performed with the financial support of the National Sciences and Engineering Research Council of Canada. We thank D Hennecart of the Université de Caen/ISMRa for making his computer code of the Niehaus model available to us.

References

Aumayr F, Fehringer M and Winter H 1984 *J. Phys. B: At. Mol. Phys.* **17** 4185
Beijers J P M, Hoekstra R and Morgenstern R 1996 *J. Phys. B: At. Mol. Opt. Phys.* **29** 1397
Brazuk A, Dijkkamp D, Drentje A G, de Heer F J and Winter H 1984b *J. Phys. B: At. Mol. Opt. Phys.* **17** 2489
Brazuk A, Winter H, Dijkkamp D, Boellaard A, de Heer F J and Drentje A G 1984a *Phys. Lett.* A **101** 139
Dijkkamp D, Brazuk A, Drentje A G, de Heer F J and Winter H 1984 *J. Phys. B: At. Mol. Phys.* **17** 4271
Folkmann F, Eisum N H, Cirić D and Drentje A G 1983 *KVI Annual Report* Groningen, The Netherlands p 63
Geller R and Jacquot B 1983 *Phys. Scr.* T **3** 19
Greenwood J B, Burns D, McCullough R W, Geddes J and Gilbody H B 1996 *J. Phys. B: At. Mol. Opt. Phys.* **29** 5867
Niehaus A 1986 *J. Phys. B: At. Mol. Phys.* **19** 2925
Wutte D, Janev R K, Aumayr F, Schneider M, Schweinzer J, Smith J J and Winter H 1997 *At. Nucl. Data Tables* **65** 155